YIELD ENHANCEMENT OF BALANCED ARMATURES THROUGH ADVANCED DATA ANALYTICS AND AI-INTEGRATED ROOT CAUSE ANALYSIS WITHIN THE LEAN SIX SIGMA FRAMEWORK

Angelito Jr. F. Manos

Research and Development – NPI Department, MedTech and Specialty Audio
Knowles Electronics (Philippines) Corporation, Cebu Light Industrial Park, Basak, Lapu-Lapu City, Cebu
AngelitoJr.Manos@knowles.com

ABSTRACT

Several manufacturing companies today struggle with delays in accurately pinpointing the root causes of issues. This often happens because they rely heavily on manual analysis tools and haven't fully adopted new technologies that could make this process faster and more adaptable. These delays can hinder efforts to reduce costs and maintain competitiveness in a rapidly evolving market. To address these challenges, organizations need to embrace smarter, more agile approaches to root cause analysis that leverage the latest technological advancements.

This paper discusses the integration of traditional problem-solving methods, such as root cause analysis and statistical tools, with AI chat models or chatbots to enhance Model X yield within the Lean Six Sigma framework. Model X, originating from mature balanced armature technology, benefits from AI-supported root cause identification techniques of historical data and insights, enabling more effective data-driven Lean Six Sigma validation of root causes. This synergy facilitates rapid pattern recognition and efficient access to relevant information. The implementation of this combined methodology has resulted in significant cost savings in Knowles' New Product Introduction (NPI) department.

1.0 INTRODUCTION

The concept of Balanced Armature (BA) drivers, a proven and mature technology, is grounded in electromagnetism. It operates by using electrical signals to vibrate a small metal reed connected to a thin metal sheet, which then produces sound in the acoustical domain (see Fig. 1).

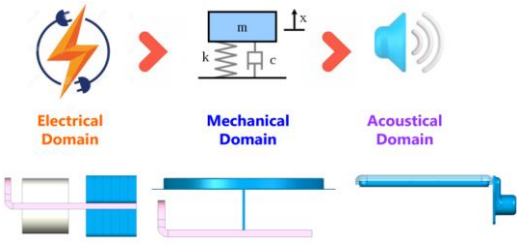

Fig. 1. Balanced Armature Driver Energy Transfer Illustration

Balanced Armature (BA) drivers are widely used in medical technology and specialty audio applications, serving as key components in devices such as hearing aids, earphones, in-ear monitors, wireless earbuds, and professional audio equipment (refer to Fig. 2).

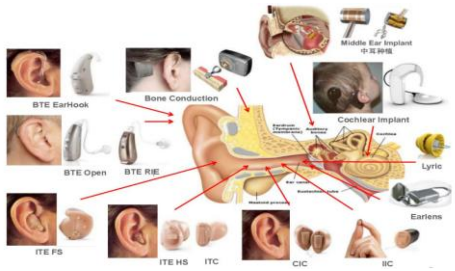

Fig. 2. Application of Balanced Armature (BA) Drivers

A balanced armature driver is made up of several essential components: the magnet, reed, coil, cup, and diaphragm (see Fig. 3). High-quality manufacturing of these components is crucial for optimal sound performance, as substandard parts can compromise sensitivity and centering precision, leading to degraded audio clarity.

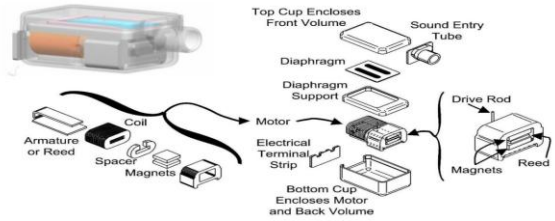

Fig. 3. Major Components of Balanced Armature (BA) Drivers

Table 1. Component Common Manufacturing Techniques

Component	Manufacturing Techniques
1. Magnet	Powder metallurgy, casting, bonding
2. Reed	Stamping, punching, laser cutting
3. Coil	Wire winding, insulation
4. Cup	Stamping, machining, injection molding
5. Diaphragm	Stamping, die cutting, lamination

Sensitivity is the ability of the balanced armature receiver to respond to sound signals, while centering ensures stable and balanced movement for consistent sound quality. Previous research has substantially advanced manufacturing processes, leading to the production of more sensitive and centered components. Building upon these innovations, the incorporation of AI chat models or chatbots with Lean Six Sigma—DMAIC methodology creates a compelling synergy.

The integration of AI chat models and chatbots into manufacturing processes offers significant advancements in root cause analysis. These intelligent systems function as diagnostic assistants, systematically identifying and suggesting potential sources of issues within production systems. By utilizing sophisticated algorithms to analyze historical data and previous research (refer to Fig. 4) [3], chatbots generate comprehensive and prioritized lists of potential root causes.

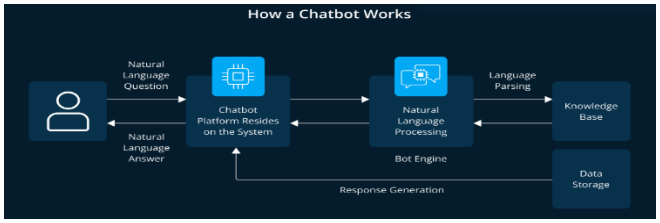

Fig. 4. How AI Chatbot Works

In this paper, AI chat models or chatbots were used alongside the Lean Six Sigma – DMAIC methodology to identify root causes. Their use greatly improved the sensitivity and stability of Model X, leading to a significant reduction in failure rates.

2.0 REVIEW OF RELATED WORK

Not applicable

3.0 METHODOLOGY

This paper employs the DMAIC methodology, incorporating the use of AI chatbots and advanced chat models to enhance analysis and solutions, thereby effectively reducing the Sensitivity and Centering failure rates of Model X.

3.1 DMAIC – Define Phase

3.1.1 Problem Statement

As shown in Fig. 5, Model X had an average yield rate of 79.5% over the past three months (October to December 2024). This is below its monthly target of 85.2% and the overall target of 93%.

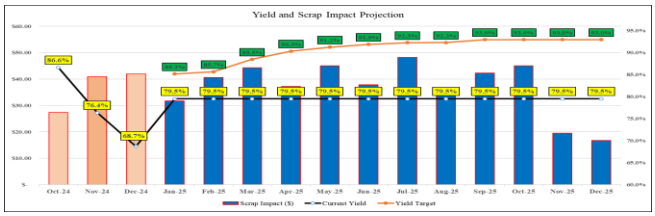

Fig. 5. Model S yield performance and target

3.1.2 Project Objective

To avoid further scrap penalties, rejection must be decreased by half to increase the yield performance of Model X from 79.5% to 90.3% by the end of March 2025.

3.2 DMAIC – Measure

3.2.1 Yield Performance

The average 3 months yield performance of Model X based on Oracle Vigilance Analytics Data is only at 79.5%, which is off by 5.7% to the January target of 85.2% (Figure 6).

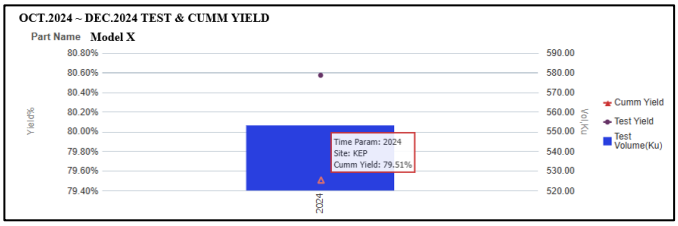

Fig. 6. Model S Yield Performance

Based on the Pareto of failures (Fig. 7), the main contributor to the low yield performance is the Failed Adjust (FA) reject, with a rejection rate of 15.48%. The 12.36% is related to sensitivity and centering issues, which account for about 90% of the overall rejects of Model X.

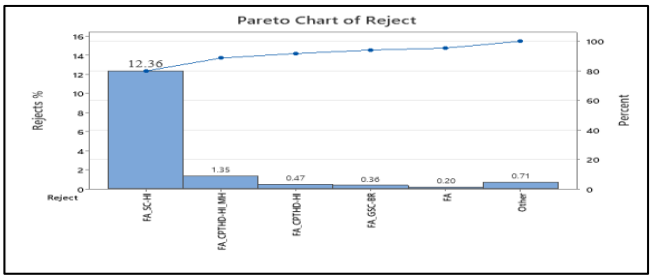

Fig. 7. Pareto of Rejects for Model X (including breakdown)

3.3 DMAIC – Analyze

On the macro process flow chart below (Fig. 8), Sensitivity and Centering issues (SC) are detected on the Adjust and Test Process, where the acoustic testing is being performed.

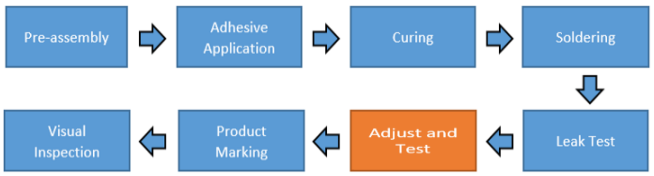

Fig. 8. Model X Process Flow Chart

To augment the list of potential root causes, an AI chatbot was tasked with retrieving and analyzing relevant research studies from existing databases and publications, utilizing natural language processing and machine learning algorithms to identify key patterns and correlations (Fig. 9).

// Generate a list of potential root causes for sensitivity and centering issues in balanced armature
// Include causes related to:
// Material: potential issues with each component (magnet, coil, diaphragm, yoke, cup) that could cause sensitivity or centering problems
// Man: possible human errors affecting assembly or handling
// Machine: issues with reed welding machine and motor to cup laser welding that could lead to sensitivity or centering problems
// Method: any process-related issues
// Environment: environmental factors affecting sensitivity and centering performance of balanced armature receivers
// Measurement: measurement inaccuracies impacting sensitivity and centering performance of balanced armature receivers
//Tabulated the results

Certainly! Here's the information organized into a clear table format:

Category	Potential Root Causes
Material	**Magnet:** - Variations in magnet strength or magnetization inconsistent with specifications - Magnet defects or impurities affecting magnetic flux - Magnet misalignment within the BA assembly **Coil:** - Incorrect wire gauge or material affecting electromagnetic response - Winding inconsistencies or defects - Insufficient insulation or insulation damage **Diaphragm:** - Material fatigue or degradation - Variations in thickness or tension - Contamination or debris **Yoke:** - Improper material or dimensions - Misalignment or deformation **Cup:** - Variations in material or surface finish - Damage or deformation causing miscentering
Human/Operator	**Assembly Errors:** - Incorrect component positioning or alignment - Excessive or insufficient force during assembly - Handling variability leading to damage **Handling/Storage:** - Contamination or moisture exposure - Improper storage causing degradation **Quality Control:** - Inconsistent inspection - Unintentional component damage during handling
Machine	**Welding Equipment:** - Incorrect welding parameters - Misalignment during welding - Equipment malfunction **Laser Welding:** - Improper calibration - Misalignment of laser focus - Vibration affecting weld quality **General Equipment:** - Wear and tear of tools - Insufficient maintenance causing variability
Method/Process	**Process Variations:** - Deviations from SOP - Lack of process controls **Tolerances:** - Variations affecting fit and alignment - Sourcing inconsistencies **Calibration:** - Inaccurate calibration affecting placement and assembly
Environmental	- Temperature extremes affecting materials or processes - High humidity leading to corrosion or moisture absorption - Dust, particles, or contaminants interfering with assembly - External vibrations/shocks impacting alignment - Air quality affecting sensitive components
Measurement	- Inaccurate instrument calibration - Inconsistent measurement techniques - Data recording errors - Non-standardized testing fixtures/setup - Environmental factors impacting measurement accuracy

Generate a list of possible root causes for sensitivity and centering issues in balanced armature components (magnet, coil, diaphragm, yoke, cup). Include causes related to:

Material: problems with each component that could cause sensitivity or centering issues
Man: human errors during assembly or handling
Machine: issues with reed welding and laser welding of the cup to the motor
Method: process-related problems
Environment: environmental factors affecting performance
Measurement: inaccuracies in measurement or inspection

Regenerate Delete

Fig. 9. Command text and Generated AI Output File (Root Cause List)

This analysis was then integrated into the Fishbone Diagram (Fig. 10) and combined with inputs from the Cross-Functional Team brainstorming, PFMEA, and lessons learned from other models, to generate a comprehensive list of potential root causes based on the various 5Ms + 1E (measurement, material, man, method, machine, environment).

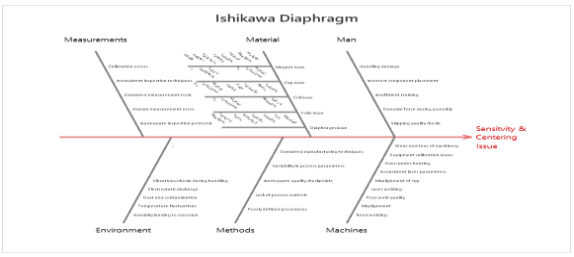

Fig. 10. Fishbone Diagram for Sensitivity NG using Minitab

After listing the potential root causes from the AI-generated list and cross-referencing with the CFT, a screening process was conducted utilizing AI assistance (Fig.11).

// Based on the factors above, screen out the root causes to be prioritized for validation.
// Rate each cause from (1) as the lowest likelihood to (5) as the highest likelihood of occurrence.
// Rate each cause from (1) as the lowest complexity to (5) as the highest complexity of validation.
// Apply weighted bias in descending order: material (5), machine, man, method, environment (1).
// Multiply the likelihood rating by the complexity rating.
// Generate a top list of priorities for validation (tabulated).

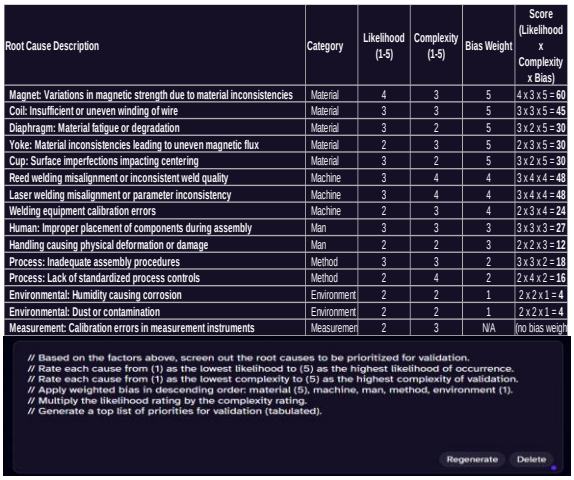

Root Cause Description	Category	Likelihood (1-5)	Complexity (1-5)	Bias Weight	Score (Likelihood x Complexity x Bias)
Magnet: Variations in magnetic strength due to material inconsistencies	Material	4	3	5	4 x 3 x 5 = 60
Coil: Insufficient or uneven winding of wire	Material	3	3	5	3 x 3 x 5 = 45
Diaphragm: Material fatigue or degradation	Material	3	2	5	3 x 2 x 5 = 30
Yoke: Material inconsistencies leading to uneven magnetic flux	Material	2	3	5	2 x 3 x 5 = 30
Cup: Surface imperfections impacting centering	Material	3	2	5	3 x 2 x 5 = 30
Reed welding misalignment or inconsistent weld quality	Machine	3	4	4	3 x 4 x 4 = 48
Laser welding misalignment or parameter inconsistency	Machine	3	4	4	3 x 4 x 4 = 48
Welding equipment calibration errors	Machine	2	3	4	2 x 3 x 4 = 24
Human: Improper placement of components during assembly	Man	3	3	3	3 x 3 x 3 = 27
Handling causing physical deformation or damage	Man	2	2	3	2 x 2 x 3 = 12
Process: Inadequate assembly procedures	Method	3	3	2	3 x 3 x 2 = 18
Process: Lack of standardized process controls	Method	2	4	2	2 x 4 x 2 = 16
Environmental: Humidity causing corrosion	Environment	2	2	1	2 x 2 x 1 = 4
Environmental: Dust or contamination	Environment	2	2	1	2 x 2 x 1 = 4
Measurement: Calibration errors in measurement instruments	Measurement	2	3	N/A	(no bias weight

// Based on the factors above, screen out the root causes to be prioritized for validation.
// Rate each cause from (1) as the lowest likelihood to (5) as the highest likelihood of occurrence.
// Rate each cause from (1) as the lowest complexity to (5) as the highest complexity of validation.
// Apply weighted bias in descending order: material (5), machine, man, method, environment (1).
// Multiply the likelihood rating by the complexity rating.
// Generate a top list of priorities for validation (tabulated).

Regenerate Delete

Fig. 11. Command text Generated AI Output File (Screening Root Cause)

Upon receiving the AI-generated list of screened potential root causes (Fig. 11), a cross-functional team conducted a cross-referencing and screening process. Each root cause was rated on a scale from 1 (least likely to occur and simplest to validate) to 5 (most likely to occur and most complex to validate).

Causes with a combined score (product of likelihood and complexity ratings) of 15 or higher were prioritized for validation, as shown in Table 2.

Table 2. Potential Root Cause Screening Prioritization

Factor	Potential Root cayse	Rating	Score
Material	Magnet Variations in magnetic strength due to material inconsistencies	VV	25
Material	Yoke Material inconsistencies leading to uneven magnetic flux	VS	15
Material	Diaphragm Material fatigue or degradation	SV	15
Machine	Mechanical Misalignment of Reed	SS	9
Machine	Laser welding Quality and Inconsitency	SS	9
Machine	Welding equipment calibration errors	NV	5
Process	Reed Deformation or damage during assembly	NV	5
Process	Lack of Standardized process in reed weld	NV	5

Occurrence	Score	Complexity	Score
V- Very Likely	5	V- Very Easy	5
S-Somewhat Likely	3	S-Somewhat Easy	3
N - Not Likely	1	N - Not Easy	1

3.3.1 Root Cause Validation

3.3.1.1 Magnet: Variations in magnetic strength due to material inconsistencies

In balanced armature receivers, the magnet is responsible for generating the magnetic flux needed to actuate the armature. Theoretical analysis indicates that optimizing key magnet dimensions—specifically thickness, surface area, and overall size—can significantly enhance flux density.

The product design is based on a balanced armature receiver concept (Fig. 12), where the magnet is used as the mechanical part that moves the reed when the coil is energized.

Therefore, a thorough reevaluation of these dimensional parameters across all magnet suppliers is required to identify potential variations. Such variations may be associated with decreased sensitivity in Model X.

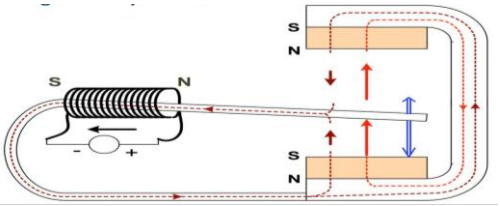

Fig. 12. Magnet, magnetic flux, coil and reed interaction

3.3.1.2 Data Gathering

Six months of magnet dimension data per lot from all suppliers were collected through the Material and Assembly Parameter Tableau Monitoring. This data was correlated with the corresponding sensitivity readings (failure rates) per supplier lot obtained from the Vigilance Analytics Multilevel Scorecard of Model X. (See Appendices A.1 & A.2)

3.3.1.3 Validation

3.3.1.3.1 Normality Test

Normality testing (Fig. 13) showed that the P-value for Magnet Surface Area of Supplier A is 0.3835, which is higher than the alpha level of 0.05. Therefore, we fail to reject the null hypothesis (Ho) and conclude that the data for surface welding area (Supplier A) follows a normal distribution.

The other three tests—magnet thickness (Supplier A), magnet thickness (Supplier B), and surface area (Supplier B)—had P-values of 0.013, 0.0005, and 0.009, respectively, indicating that these data do not follow a normal distribution.

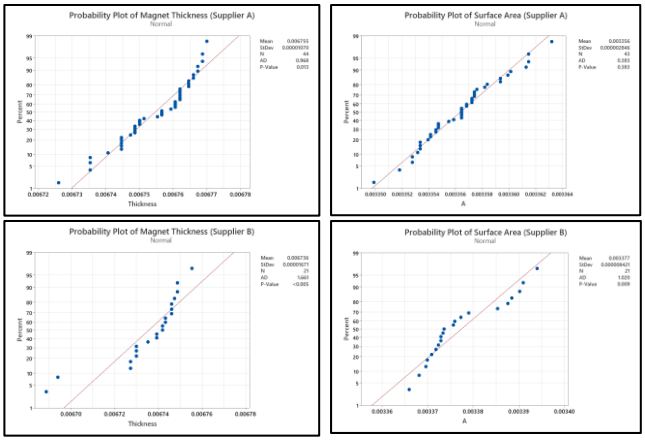

Fig. 13. Probability Plot of Magnet Thickness & Magnet Surface Area Supplier A and B

3.3.1.3.2 Regression Analysis

The multiple regression model for both Magnet Supplier A and B, examining magnet thickness and surface area dimensions (as shown in Figure 14), has P-values of 0.531 and 0.290, respectively. Since these P-values are higher than the alpha level of 0.05, we fail to reject the null hypothesis (Ho). This indicates that there is no statistically significant relationship between Sensitivity NG rejection and the magnet thickness or surface area for either supplier.

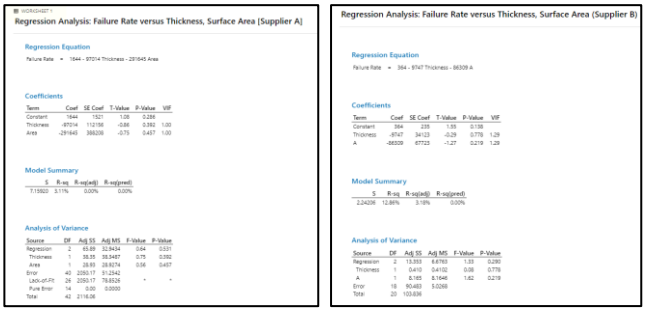

Fig. 14. Multiple Regression Analysis Results for Magnet Supplier A and Supplier B: Magnet Thickness, Surface Area, and Sensitivity NG Failure Rate

3.3.1.4. Root Cause Conclusion

Based on the statistical analysis conducted, it is concluded that variations in magnet thickness and surface dimensions across the two suppliers are not valid root causes of Sensitivity NG (FA) rejection.

3.3.2.1 Material: Yoke material dimension inconsistencies leading to uneven magnetic flux

The yoke provides structural support for the coil, reed, magnet, and diaphragm, ensuring stable operation. It also completes the magnetic circuit and guides magnetic flux (Fig.

12), which is crucial for optimizing the sensitivity and performance of the balanced armature transducer.

Critical dimensions—length, width, flatness, and cross-sectional gaps (Fig. 15)—determine how efficiently the yoke channels and concentrates magnetic flux, affecting the magnetic circuit's completion and sensitivity, while minimizing reluctance and flux leakage.

Therefore, a thorough reevaluation of these dimensions is necessary to identify potential variations that may reduce sensitivity in Model X.

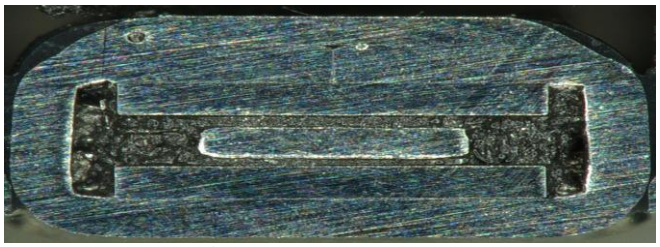

Fig. 15. Cross-section of yoke-magnet-reed assembly

3.3.2.2 Data Gathering

One year of yoke dimension data per lot was collected through the Material and Assembly Parameter Tableau Monitoring (Fig. 16). This data was correlated with the corresponding sensitivity readings (failure rates) for each arrival lot, obtained from the Vigilance Analytics Multilevel Scorecard of Model X (Fig. 17). Key yoke dimensions were statistically tested to identify significant correlations with the sensitivity failure rate of Model X. See Appendix B

Fig. 16. Tableau IQC Measurement (Knowles-exclusive Monitoring System)

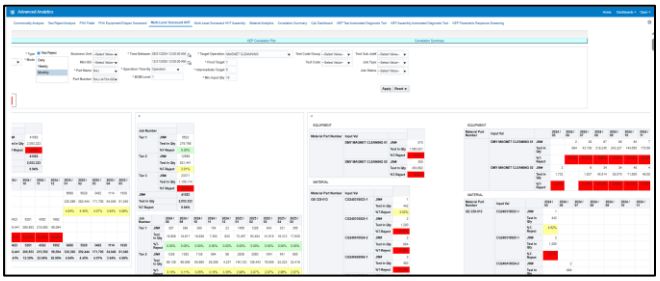

Fig.17 Vigilance Analytics (Knowles-exclusive) Multi-level Scorecard

3.3.2.3 Validation

3.3.2.3.1 Normality Test

Normality testing (Fig. 18) showed that the P-values for Yoke Gap and Window Width A are 0.504 and 0.886, respectively, both exceeding the significance level of 0.05. Therefore, the test fails to reject the null hypothesis (H_0), indicating that the data for Yoke Gap and Window Width on both materials follow a normal distribution.

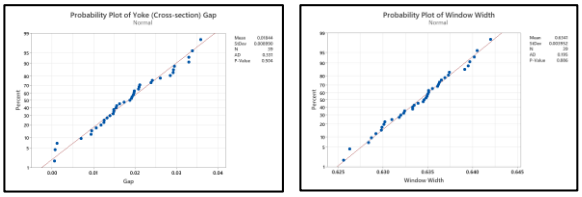

Fig. 18. Probability Plot of Yoke Critical Dimensions – Gap & Width

Normality testing (Fig. 19) for the remaining yoke critical dimension showed P-values of 0.015 and 0.049, both below 0.05. Therefore, the test reject Null Hypothesis (H_0) and conclude that the data for gap and width are non-normal.

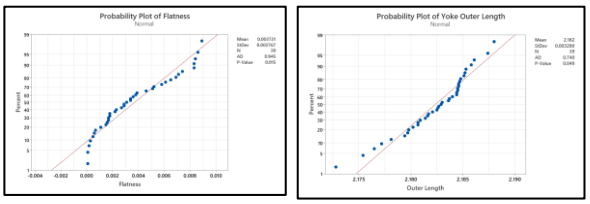

Fig. 19. Probability Plot of Yoke Critical Dimensions: Flatness & Length

3.3.2.3.2 Regression Analysis

The multiple regression model for yoke dimensions, examining gap, outer length, window width, and flatness (as shown in Fig. 20) against Model X Sensitivity NG reading, showed P-values of 0.000, 0.952, 0.138, and 0.571, respectively. Since the P-value for gap (0.000) is less than the alpha level of 0.05, the null hypothesis (H_0) is rejected. This indicates a statistically significant relationship between the yoke cross-sectional gap dimension and Sensitivity NG rejection.

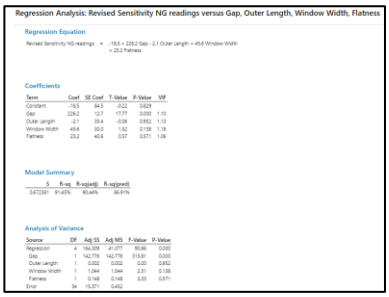

Fig. 20. Multiple Regression Analysis Results for yoke critical dimension gap, outer length, width and flatness against Sensitivity NG Failure Rate

3.3.2.4 Root Cause Conclusion

It is concluded that the yoke dimension, specifically the gap, is a valid root cause of Sensitivity NG rejection.

3.3.3.1 Material: Diaphragm material fatigue and Assembly issue.

A BA driver is essentially a complicated Spring-Mass system (Fig. 21) where:

Mass (m) = amount of "stuff" that moves,
Stiffness (k) = summation of all "springs" in the system
Damping (B) = friction and other losses
Force (f) = the electric signal moving on the coil
Distance (x) = the displacement of armature

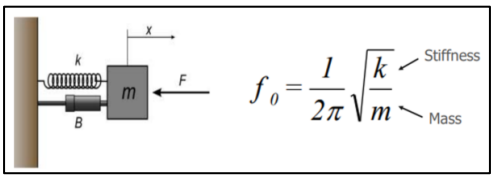

Fig. 21. Illustration of Spring-Mass System

In a spring-mass system, the diaphragm is the movable part that responds to external forces. A no-good (NG) condition occurs when the diaphragm's movement is distorted or less efficient, often due to material fatigue, deformation, or improper attachment to parts like the cup or casing.

3.3.3.2 Data Gathering

During the failure analysis, it was observed that the bad units exhibit a slight floating diaphragm condition compared to the good units, as shown in Fig. 22. It is important to note that these visual observations are not included in the current visual inspection criteria.

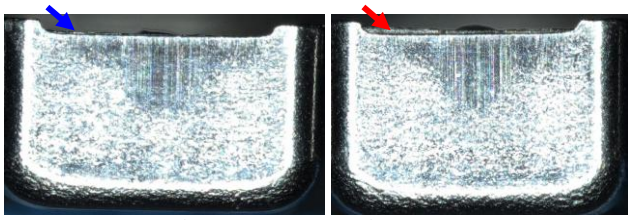

Fig. 22. Illustration of Good and Bad unit (floating diaphragm)

Additionally, to assess the sensitivity of balanced armature receivers, a headroom test is performed. The headroom test primarily evaluates the maximum sensitivity the unit can handle without distortion, compared to a standard reference, which is related to the diaphragm's ability to move freely at higher signal levels.

A headroom test (Appendix B) is conducted in each unit for further verification.

3.3.3.3 Validation

3.3.3.3.1 Normality Test

The results shown in Figure 23 indicate that the P-values for headroom in both Good units and Bad units are 0.005, which are lower than the set alpha level of 0.05. Therefore, the test rejects the null hypothesis (Ho) and confirms that the data collected for headroom in both units follow a non-normal distribution.

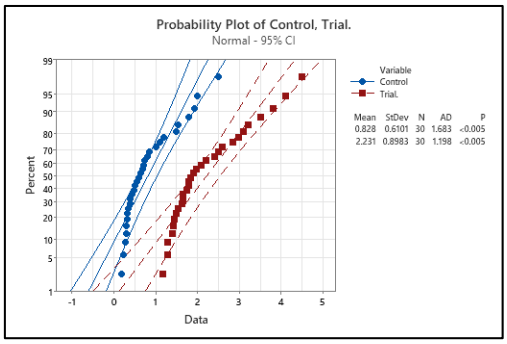

Fig 23: Normality test for Headroom of Good and Bad units

3.3.3.3.2 Hypothesis Testing – Mann-Whitney

Performing a Mann-Whitney test (Fig. 24) resulted in a P-value of 0.000, which is lower than the set alpha level of 0.05. Therefore, the test rejects the null hypothesis (Ho) and confirms that there is a significant difference between the mean headroom of Good units and Bad units.

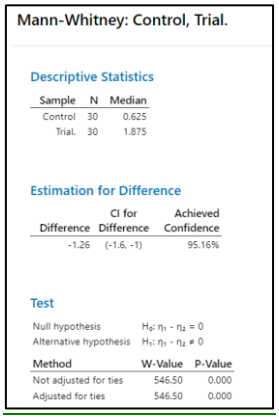

Fig 24. Hypothesis Testing – Mann-Whitney (Non-Normal Distribution) for Headroom of Good and Bad units

3.3.3.4 Conclusion

It is concluded that the floating diaphragm condition is a valid root cause for Sensitivity NG rejection.

4.0 RESULTS AND DISCUSSION

4.1 Root Cause Validation Summary

After a series of validation activities, there were remaining two (2) valid Potential Root Causes as shown in Table 3. The other validation results of the other factors can be found in the Appendix Section 10.2.

Table 3. Root Cause Validation Table Summary

Element	Potential Root Causes	Verification	Target	Result	Status	Remarks
Method	Human reed open size measurement error		10-Dec	Invalid	Closed	Operator passed the MSA.
Material	Yoke material inconsistencies leading to uneven magnetic flux		12-Dec	Valid	Closed	Yoke gap is a concern.
Environment	Humidity fluctuations		11-Dec	Invalid	Closed	No fluctuations observed in the control chart.
Machine	Laser welding quality and inconsistency		01-Dec	Invalid	Closed	No fluctuations observed in pull test data.
Man	Poor operator work quality		02-Dec	Invalid	Closed	Veteran operators are running on the line.
Material	Diaphragm material fatigue or degradation		03-Dec	Valid	Closed	Floating on the cup is a concern.
Machine	MTC welding equipmentstability issue		05-Dec	Invalid	Closed	No fluctuations in motor to case gap on yoke window
Method	Incorrect ESPC inspection technique: Reed length		07-Dec	Invalid	Closed	No fluctuations in reed length measurement
Material	Misalignment of the yoke		09-Dec	Invalid	Closed	No fluctuations observed in C-value data.
Environment	Temperature fluctuations		11-Dec	Invalid	Closed	No fluctuations observed in the control chart.
Material	Magnet variations in magnetic strength due to material inconsistencies		12-Dec	Invalid	Closed	Regression analysis shows no significant p-value.
Method	Lack of a standardized process in reed welding		01-Dec	Invalid	Closed	Camera alignment is OK.
Machine	Mechanical misalignment of the reed		02-Dec	Invalid	Closed	No fluctuations observed in open size measurements.
Machine	Coupler setup issues during adjustment and testing		03-Dec	Invalid	Closed	Correctly adjusted and tested the coupler.
Material	Reed deformation or damage during assembly		05-Dec	Invalid	Closed	No fluctuations observed in reed open size.

4.2 DMAIC – Improve

4.2.1 Material: Yoke gap dimension inconsistencies

Using the SCAMPER method (Fig. 25), the yoke design was modified from a direct stamped folded yoke to an interlocked stamped folded yoke to eliminate the yoke gap and address the inherent dimensional inconsistency of the material.

SCAMPER	Proposal	Responsible
Substitute		
Combine		
Adapt		
Modify	Modify the yoke design 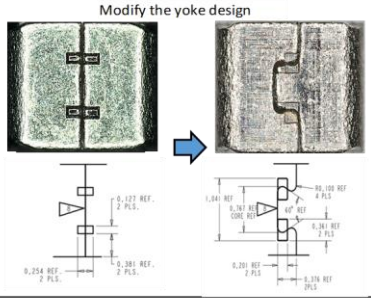	Jun Manos
Put to Other Uses		
Eliminate		
Rearrange		

Fig. 25. SCAMPER Table for Yoke Design Improvement

4.2.1.1 Validation

The electroacoustic adjustment graph in Fig. 26 shows the sensitivity comparison between the current yoke design and the new interlock yoke design. It is observed that the sensitivity of the last hit for the new yoke design is significantly improved compared to the current design.

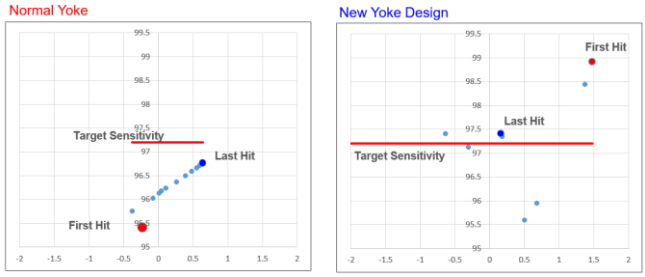

Fig. 26. Electroacoustic Adjustment Graph of Model X Comparing the Current Yoke Design and the New Interlock Yoke Design.

4.2.1.1.1 Normality Test

Additionally, a headroom test was performed to measure the maximum sensitivity between the two yoke designs. See Appendix D. Normality testing (Fig. 27) for the headroom yielded p-values of 0.015 and 0.049, both of which are above the significance level of 0.05. Therefore, the test failed to reject the null hypothesis (H_0), indicating that the data for the headroom are normally distributed.

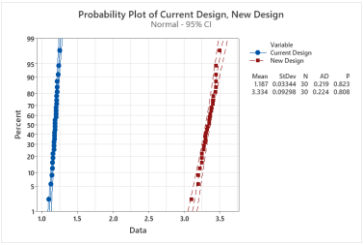

Fig. 27. Normality Test of Headroom Data for Current vs. New Design

4.2.1.1.2 Hypothesis Test

Based on the results of the two-tailed t-test (Fig. 28), there is a statistically significant difference between the two yoke designs in terms of headroom, as the p-value is less than the significance level of 0.05. Therefore, we reject the null hypothesis and conclude that the headroom measurements differ significantly between the two designs.

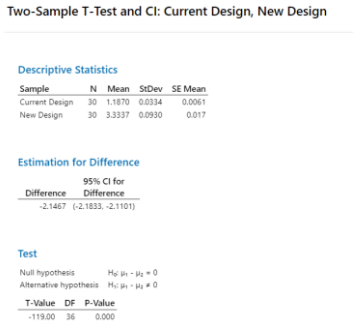

Fig. 28. Hypothesis Testing: Two-Sample t-Test of Headroom Data for Current vs. New Design

4.2.1.1.3 Evaluation Run

After a series of reliability and tolerance analyses, as well as trial runs, the new yoke design was implemented into the production line, along with the corresponding improvement rate shown in Fig. 29.

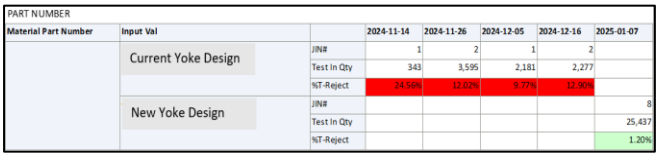

Fig 29. Vigilance Analytics Multilevel Scorecard (Sensitivity NG) Trend

4.2.2 Diaphram Assembly Issue: Floating Diaphragm

Using the SCAMPER method (Fig. 30), we introduced a width measurement output during diaphragm and cup assembly to precisely control the dimensions, addressing the absence of a specific assembly dimension standard for the cup, even though one exists for OPD.

However, despite having the OPD specifications, the actual performance was not fully aligned. To resolve this, we established a new measurement specification for the cup and diaphragm widths, which effectively prevents floating diaphragms and enhances manufacturing process stability.

SCAMPER	Proposal	Responsible
Substitute		
Combine		
Adapt	Adapt the new width measurement method for the cup assembly. 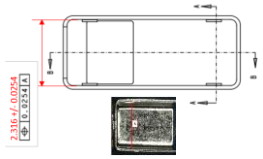	Jun Manos
Modify	Modify the measurement specification for the OPD width 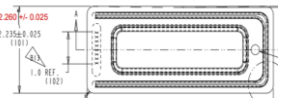	Jun Manos
Put to Other Uses		
Eliminate		
Rearrange		

Fig. 30. SCAMPER Table for Cup & OPD Improvement

4.2.2.1 Validation

The headroom test results, obtained using the newly established limits for the cup and diaphragm assembly widths, were characterized and analyzed based on the configurations listed in Table 4, which detail the minimum and maximum dimensional bounds. These results were further validated through equivalent headroom testing to ensure robustness across the defined dimensional range with good process capability (Fig. 31). See Appendix E for the headroom test data of four runs.

Table 4. New Width Measurement Min-Max Characterization Table

Run	Cup Width	Diaphragm Width	Description
1	2.291 (min)	2.235 (min)	Both at minimum levels
2	2.291 (min)	2.285 (max)	Cup at min, diaphragm at max
3	2.341 (max)	2.235 (min)	Cup at max, diaphragm at min
4	2.341 (max)	2.285 (max)	Both at maximum levels

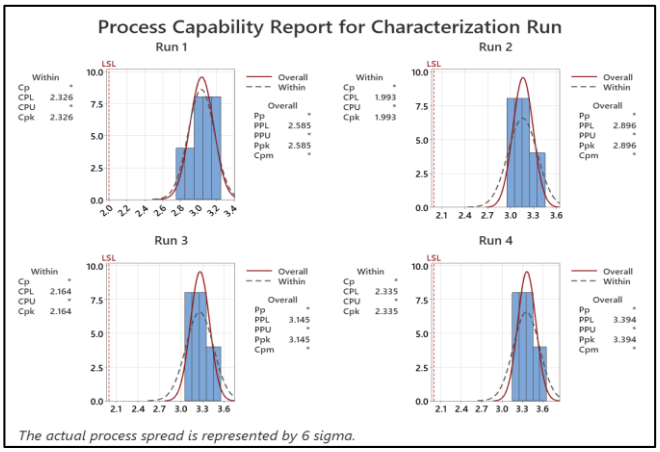

Fig. 31. Process Capability of Headroom Test for 4 Characterization Runs

4.2.2.2 Evaluation Run

After a series of reliability and tolerance analyses, as well as trial runs, the new specification was implemented into the production line, along with the corresponding improvement rate shown in Figure 32.

Model X	Input Val		2024-12-16	2024-12-18	2024-12-21	2024-12-22	2024-12-23	2024-12-26	2025-01-03	2025-01-04
	OLD SPECIFICATION	JIN#	4	11	15	9	7			
		Test In Qty	3,607	7,449	18,229	8,389	5,457			
		%T-Reject	9.69%	10.20%	6.70%	13.00%	8.39%			
	NEW SPECIFICATION	JIN#						10	10	10
		Test In Qty						13,296	6,783	10,321
		%T-Reject						2.31%	1.35%	2.50%

Fig. 32. Model X Sensitivity NG (SC-HI) Rejection Trend using Vigilance Analytics Multilevel Scorecard

A series of validations and improvements led to a reduction of Sensitivity NG rejection from 20.13% to 1.94%, which is a total of 90.36% improvement as shown in Fig. 33.

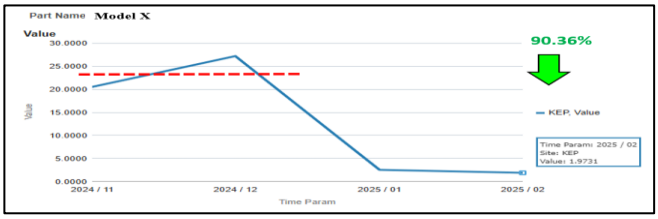

Fig. 33. Model X, Sensitivity NG (SC-HI) Rejection Trend (November 2024 to February 2025)

This contributes to an increase in yield rate for Model from 79.5% to 94.22%, which is a total of 15.62% improvement as shown in Fig. 34.

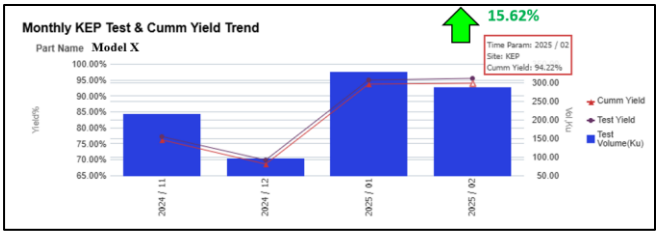

Fig. 34. Model X Yield Trend (Nov,2024 to Feb, 2025)

The improvements helped the company save $36,401.32 for scrap cost avoidance.

4.3 DMAIC – Control

Following root cause analysis and corrective actions, all lessons learned and implemented measures have been standardized and documented. The yoke design print has been updated to reflect the revised specifications (Fig. 35).

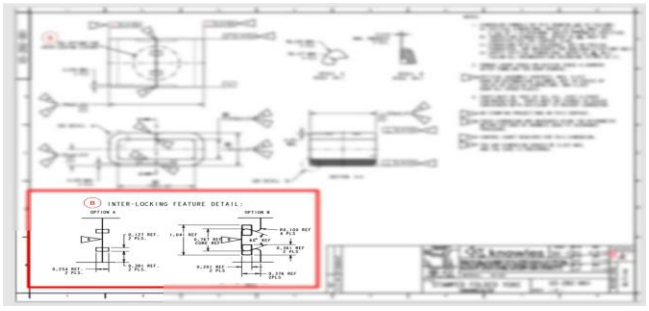

Fig. 35. Updated Prints of New Yoke Design

In addition, the new dimension's prints of cup and diaphragm assembly (Fig. 36) have also been updated.

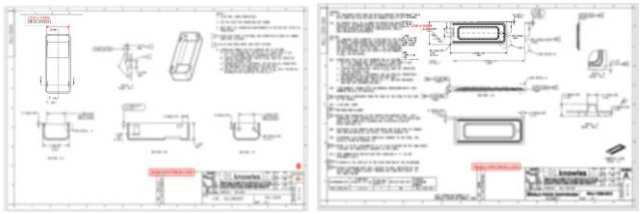

Fig. 36. Updated marked up Sub-Assembly Prints

5.0 CONCLUSION

The objective to reduce the rejection rate of Sensitivity NG (SC-HI) on the Model S balanced armature driver by half was successfully achieved through advanced data analytics and the integration of AI chat models or chatbots, alongside the Lean Six Sigma methodology. This was accomplished by improving the yoke design and effectively optimizing the assembly dimension specifications, leading to a significant reduction in the Sensitivity NG (SC-HI) failure rate.

6.0 RECOMMENDATIONS

It is highly recommended to integrate AI chatbot tools within the DMAIC (Define, Measure, Analyze, Improve, Control) framework to enhance root cause validation for similar manufacturing firms where rapid problem resolution is critical. Specifically, AI chatbots can assist manufacturing engineers by listing all potential root causes derived from mature technologies, thereby enabling more efficient identification and screening of probable causes prior to factor validation. Furthermore, it is essential to employ a structured analysis approach that leverages AI-supported root cause identification techniques and Lean Six Sigma statistical tools throughout the root cause validation process.

7.0 ACKNOWLEDGMENT

The author would like to thank the Cross-Functional Team (CFT), including the Operators, Technicians, and Engineers, for extending support on this project, as well as the Management Team of Knowles Electronics (Philippines) Corporation for the unwavering support on this project.

8.0 REFERENCES

1. Knowles Electronics, LLC, Itasca, IL, USA, (2023). What is Balanced Armature? https://www.knowles.com/applications/ear-solutions/premium-sound/what-is-balanced-armature

2. LibreTexts Physics, California State University, (2023). The Motion of a Spring-Mass System https://phys.libretexts.org/Bookshelves/University_Physics/

3. How AI Chatbot Works https://www.leewayhertz.com/ai-chatbots/

9.0 ABOUT THE AUTHOR

Angelito Manos, Jr. is a graduate of Ateneo De Cagayan, Xavier University and a licensed Electronics and Communication Engineer. He has been a Process Engineer at the Micro Actuator Technology Division of MinebeaMitsumi Inc. for 7 years and is an Advanced Manufacturing Engineer at the MedTech and Specialty Audio (MSA) segment of Knowles Electronics Philippines for 3 years. He is a Certified Lean Six Sigma Black Belt and a TRIZ Level 1 Practitioner.

10.0 APPENDICES

10.1 Tables and Raw Data

APPENDIX A.1 SUPPLIER A

Date Arrived/ Supplier / Lot #	Date Arrived	Lot	Thickness	L1	L2	A	Failure Rate
2024-08-01 - XW240801001S	2024-08-01	XW240801001S	0.00669	0.05804	0.05800	0.00337	7.4
2024-08-08 - XW240808002S	2024-08-08	XW240808002S	0.00669	0.05806	0.05804	0.00337	6.0
2024-08-14 - XW240814003S	2024-08-14	XW240814003S	0.00674	0.05814	0.05812	0.00338	5.2
2024-08-21 - XW240821004S	2024-08-21	XW240821004S	0.00673	0.05806	0.05808	0.00337	9.0
2024-08-30 - XW240830005S	2024-08-30	XW240830005S	0.00673	0.05808	0.05804	0.00337	9.0
2024-09-05 - XW240905001S	2024-09-05	XW240905001S	0.00674	0.05803	0.05805	0.00337	6.0
2024-09-12 - XW240912002S	2024-09-12	XW240912002S	0.00673	0.05808	0.05807	0.00337	9.0
2024-09-20 - XW240920003S	2024-09-20	XW240920003S	0.00673	0.05809	0.05812	0.00338	8.1
2024-09-26 - XW240926004S	2024-09-26	XW240926004S	0.00673	0.05810	0.05813	0.00338	8.1
2024-10-08 - XW241008001S	2024-10-08	XW241008001S	0.00675	0.05819	0.05823	0.00339	8.1
2024-10-11 - XW241011002S	2024-10-11	XW241011002S	0.00674	0.05809	0.05807	0.00337	8.1
2024-10-16 - XW241016003S	2024-10-16	XW241016003S	0.00674	0.05813	0.05807	0.00338	8.1
2024-10-23 - XW241023004S	2024-10-23	XW241023004S	0.00675	0.05806	0.05807	0.00337	8.1
2024-10-30 - XW241030005S	2024-10-30	XW241030005S	0.00675	0.05806	0.05804	0.00337	8.1
2024-11-07 - XW241107001S	2024-11-07	XW241107001S	0.00674	0.05824	0.05822	0.00339	8.1
2024-11-13 - XW241113002S	2024-11-13	XW241113002S	0.00675	0.05821	0.05815	0.00339	8.1
2024-11-21 - XW241121003S	2024-11-21	XW241121003S	0.00676	0.05818	0.05797	0.00337	2.9
2024-11-27 - XW241127004S	2024-11-27	XW241127004S	0.00675	0.05824	0.05821	0.00339	3.1
2024-12-04 - XW241204001S	2024-12-04	XW241204001S	0.00674	0.05809	0.05808	0.00337	3.1
2024-12-11 - XW241211002S	2024-12-11	XW241211002S	0.00675	0.05816	0.05825	0.00339	4.5
2024-12-19 - XW241219003S	2024-12-19	XW241219003S	0.00674	0.05826	0.05826	0.00339	2.0

APPENDIX A.2 SUPPLIER B

Date Arrived/ Supplier / Lot #	Date	Lot	Thickness	L1	L2	A	Failure Rate
2024-08-07 - CG240508910-2	2024-08-07	CG240508910-2	0.00676	0.05797	0.05798	0.00336	6.6
2024-08-07 - CG240522035-1	2024-08-07	CG240522035-1	0.00676	0.05787	0.05788	0.00335	10.0
2024-08-07 - CG240522036-1	2024-08-07	CG240522036-1	0.00675	0.05792	0.05790	0.00335	6.0
2024-08-13 - CG240522036-2	2024-08-13	CG240522036-2	0.00675	0.05792	0.05790	0.00335	6.0
2024-08-13 - CG240522037-1	2024-08-13	CG240522037-1	0.00673	0.05765	0.05755	0.00332	10.0
2024-08-13 - CG240522037-2	2024-08-13	CG240522037-2	0.00674	0.05792	0.05791	0.00335	10.0
2024-08-22 - CG240522037-3	2024-08-22	CG240522037-3	0.00674	0.05792	0.05791	0.00335	10.0
2024-08-22 - CG240528943-1	2024-08-22	CG240528943-1	0.00677	0.05792	0.05790	0.00335	7.6
2024-08-22 - CG240528944-1	2024-08-22	CG240528944-1	0.00676	0.05793	0.05794	0.00336	14.7
2024-08-28 - CG240528944-2	2024-08-28	CG240528944-2	0.00676	0.05793	0.05794	0.00336	14.7
2024-08-28 - CG240614021-1	2024-08-28	CG240614021-1	0.00674	0.05795	0.05795	0.00336	13.7
2024-08-28 - CG240614022-1	2024-08-28	CG240614022-1	0.00676	0.05794	0.05794	0.00336	4.3
2024-09-05 - CG240614022-2	2024-09-05	CG240614022-2	0.00676	0.05794	0.05794	0.00336	4.3
2024-09-05 - CG240619925-1	2024-09-05	CG240619925-1	0.00676	0.05796	0.05794	0.00336	7.5
2024-09-05 - CG240619926-1	2024-09-05	CG240619926-1	0.00677	0.05798	0.05797	0.00336	5.3
2024-09-12 - CG240619926-2	2024-09-12	CG240619926-2	0.00677	0.05798	0.05797	0.00336	5.3
2024-09-12 - CG240627942-1	2024-09-12	CG240627942-1	0.00677	0.05788	0.05794	0.00335	9.7
2024-09-12 - CG240627943-1	2024-09-12	CG240627943-1	0.00677	0.05789	0.05792	0.00335	6.0
2024-09-24 - CG240703904-2	2024-09-24	CG240703904-2	0.00677	0.05794	0.05792	0.00336	9.0
2024-09-24 - CG240703905-1	2024-09-24	CG240703905-1	0.00676	0.05790	0.05791	0.00335	9.0
2024-10-07 - CG240703905-2	2024-10-07	CG240703905-2	0.00676	0.05790	0.05791	0.00335	9.0
2024-10-07 - CG240711913-1	2024-10-07	CG240711913-1	0.00675	0.05794	0.05795	0.00336	9.0
2024-10-07 - CG240711914-1	2024-10-07	CG240711914-1	0.00676	0.05792	0.05792	0.00335	7.5
2024-10-15 - CG240711914-2	2024-10-15	CG240711914-2	0.00676	0.05792	0.05792	0.00335	7.5
2024-10-22 - CG240711914-3	2024-10-22	CG240711914-3	0.00676	0.05792	0.05792	0.00335	7.5
2024-10-22 - CG240717923-1	2024-10-22	CG240717923-1	0.00677	0.05797	0.05797	0.00336	18.1
2024-10-22 - CG240717924-1	2024-10-22	CG240717924-1	0.00676	0.05799	0.05799	0.00336	9.0
2024-10-22 - CG240731956-1	2024-10-22	CG240731956-1	0.00675	0.05790	0.05793	0.00335	24.3
2024-10-29 - CG240731956-2	2024-10-29	CG240731956-2	0.00675	0.05790	0.05793	0.00335	24.3
2024-10-29 - CG240731957-1	2024-10-29	CG240731957-1	0.00674	0.05795	0.05797	0.00336	9.6
2024-11-06 - CG240731957-2	2024-11-06	CG240731957-2	0.00674	0.05795	0.05797	0.00336	9.6
2024-11-06 - CG240731958-1	2024-11-06	CG240731958-1	0.00674	0.05790	0.05789	0.00335	9.6
2024-11-06 - CG240813923-1	2024-11-06	CG240813923-1	0.00675	0.05793	0.05794	0.00336	32.1
2024-11-12 - CG240813923-2	2024-11-12	CG240813923-2	0.00675	0.05793	0.05794	0.00336	32.1
2024-11-12 - CG240813924-1	2024-11-12	CG240813924-1	0.00676	0.05793	0.05795	0.00336	4.9
2024-11-27 - CG240813925-2	2024-11-27	CG240813925-2	0.00675	0.05795	0.05794	0.00336	5.9
2024-11-27 - CG240829956-1	2024-11-27	CG240829956-1	0.00676	0.05793	0.05796	0.00336	3.9
2024-12-03 - CG240829956-2	2024-12-03	CG240829956-2	0.00676	0.05793	0.05796	0.00336	3.9
2024-12-03 - CG240829957-1	2024-12-03	CG240829957-1	0.00674	0.05794	0.05794	0.00336	2.9
2024-12-11 - CG240829957-2	2024-12-11	CG240829957-2	0.00674	0.05794	0.05794	0.00336	2.9
2024-12-11 - CG240919923-1	2024-12-11	CG240919923-1	0.00674	0.05792	0.05793	0.00336	2.9
2024-12-11 - CG240924935-1	2024-12-11	CG240924935-1	0.00676	0.05794	0.05793	0.00336	2.9
2024-12-18 - CG240924935-2	2024-12-18	CG240924935-2	0.00676	0.05794	0.05793	0.00336	2.9
2024-12-18 - CG241024944-1	2024-12-18	CG241024944-1	0.00675	0.05795	0.05798	0.00336	2.9

APPENDIX B YOKE KEY DIMENSIONS VS SENSITIVITY READINGS %

Lot	Gap	Outer length	Window Width	Flatness	Sensitivty NG readings
24JAN.,2024Z	0.0330	2.1754	0.6395	0.0039	13.0
25 JAN.,2024	0.0012	2.1728	0.6374	0.0003	8.0
26 JAN.,2024	0.0133	2.1781	0.6420	0.0031	9.5
29 JAN 2024	0.0125	2.1765	0.6397	0.0027	9.0
31 JAN.,2024	0.0330	2.1772	0.6345	0.0023	13.0
02 FEB.,2024	0.0006	2.1826	0.6324	0.0001	7.0
06FEB.,2024	0.0209	2.1837	0.6405	0.0016	11.0
20 FEB.,2024	0.0359	2.1880	0.6362	0.0002	15.0
26FEB.,2023B	0.0339	2.1827	0.6320	0.0011	13.5
04 MAR.,2024	0.0293	2.1807	0.6365	0.0006	12.0
11 MAR.,2024	0.0140	2.1809	0.6333	0.0005	8.5
18 MAR.,2024	0.0149	2.1817	0.6402	0.0007	8.8
- 25MAR2024	0.0156	2.1802	0.6335	0.0017	9.0
01APR.,2024F	0.0149	2.1830	0.6287	0.0022	8.8
08 APR.,2024	0.0198	2.1853	0.6318	0.0001	11.0
15 APR.,2024	0.0107	2.1847	0.6310	0.0015	7.5
- 22APR2024	0.0155	2.1807	0.6323	0.0051	9.0
29 APR.,2024	0.0148	2.1798	0.6284	0.0029	8.8
13 MAY 2024	0.0188	2.1797	0.6301	0.0038	10.0
20MAY.,2024	0.0126	2.1821	0.6333	0.0034	8.0
10JUN.,2024	0.0174	2.1845	0.6369	0.0017	10.0
17 JUN.,2024	0.0199	2.1825	0.6350	0.0034	11.0
24JUN.,2024	0.0242	2.1851	0.6351	0.0069	12.5
1 JULY.,2024	0.0193	2.1794	0.6339	0.0089	10.0
08JUL.,2024B	0.0285	2.1844	0.6351	0.0046	13.0
15JUL.,2024D	0.0070	2.1874	0.6361	0.0052	6.5
2 JUL.,2024D	0.0008	2.1816	0.6299	0.0083	7.0
01 AUG 2024	0.0261	2.1836	0.6348	0.0065	12.0
05AUG.,2024	0.0094	2.1814	0.6346	0.0058	7.0
2 AUG.,2024	0.0295	2.1844	0.6355	0.0071	13.0
19 AUG 2024	0.0096	2.1852	0.6349	0.0029	7.5
- 02SEP2024	0.0192	2.1861	0.6302	0.0018	10.0
09 SEP 2024	0.0163	2.1829	0.6256	0.0086	9.0
26AUG.,2024	0.0210	2.1848	0.6298	0.0084	11.0
27 SEP 2024	0.0239	2.1840	0.6391	0.0074	12.0
07OCT.,2024E	0.0292	2.1845	0.6363	0.0083	13.0
21OCT.,2024	0.0118	2.1858	0.6263	0.0036	8.0
04NOV.,2024B	0.0212	2.1846	0.6292	0.0061	11.0
18NOV.,2024G	0.0196	2.1846	0.6373	0.0018	10.0

APPENDIX C HEADROOM TEST DATA GOOD VS BAD UNITS

Unit #	Bad units	Good units
1	0.65	3.45
2	1.02	3.2
3	0.77	3.5
4	0.45	3.1
5	0.9	3.35
6	0.85	3.25
7	0.6	3.55
8	1.15	3.3
9	0.78	3.6
10	0.55	3.15
11	0.92	3.4
12	0.7	3.2
13	0.84	3.45
14	0.68	3.5
15	0.8	3.25
16	0.9	3.35
17	0.73	3.55
18	0.88	3.3
19	0.66	3.6
20	0.77	3.15
21	0.83	3.45
22	0.69	3.2
23	0.94	3.5
24	0.72	3.1
25	0.81	3.35
26	0.59	3.25
27	0.87	3.55
28	0.65	3.3
29	0.78	3.6
30	0.83	3.15

APPENDIX D HEADROOM TEST: OLD & NEW YOKE DESIGN

Old Design	New Yoke Design
1.15	3.45
1.25	3.10
1.10	3.25
1.20	3.35
1.18	3.45
1.22	3.20
1.19	3.50
1.21	3.28
1.17	3.40
1.23	3.33
1.16	3.25
1.20	3.30
1.14	3.45
1.19	3.20
1.21	3.36
1.18	3.41
1.22	3.22
1.20	3.38
1.17	3.27
1.19	3.31
1.13	3.45
1.24	3.29
1.16	3.37
1.21	3.44
1.20	3.32
1.15	3.25
1.18	3.40
1.22	3.38
1.19	3.30
1.17	3.35

APPENDIX E HEADROOM TEST DATA CHARACTERIZATION

Gap and Dia New Specification Headroom Characterization	Run 1	Run 2	Run 3	Run 4
1	2.80	3.00	3.10	3.20
2	3.00	3.20	3.30	3.40
3	3.20	3.10	3.20	3.30
4	3.10	3.30	3.40	3.50
5	2.90	3.00	3.10	3.20
6	3.00	3.20	3.30	3.40
7	3.10	3.10	3.20	3.30
8	3.20	3.40	3.50	3.60
9	2.80	3.00	3.10	3.20
10	3.00	3.20	3.30	3.40
11	3.20	3.10	3.20	3.30
12	3.10	3.30	3.40	3.50
13	2.90	3.00	3.10	3.20
14	3.00	3.20	3.30	3.40
15	3.10	3.10	3.20	3.30
16	3.20	3.40	3.50	3.60
17	2.80	3.00	3.10	3.20
18	3.00	3.20	3.30	3.40
19	3.20	3.10	3.20	3.30
20	3.10	3.30	3.40	3.50
21	2.90	3.00	3.10	3.20
22	3.00	3.20	3.30	3.40
23	3.10	3.10	3.20	3.30
24	3.20	3.40	3.50	3.60
25	2.80	3.00	3.10	3.20
26	3.00	3.20	3.30	3.40
27	3.20	3.10	3.20	3.30
28	3.10	3.30	3.40	3.50
29	2.90	3.00	3.10	3.20
30	3.00	3.20	3.30	3.40
31	3.10	3.10	3.20	3.30
32	3.20	3.40	3.50	3.60

10.2 Other Root Cause Validation

10.2.1 Human measurement error

The Pairwise Pearson Correlation Method for Yoke Gap and Failed Adjust (FA) rejection (Figure 31) resulted in a P-Value of 0.321, which is higher than the set alpha level of 0.05, thus, the test result failed to reject the Null Hypothesis (H_o) and confirmed that the Yoke Gap does not have significant correlation and is not a valid root cause of Failed Adjust (FA) rejection.

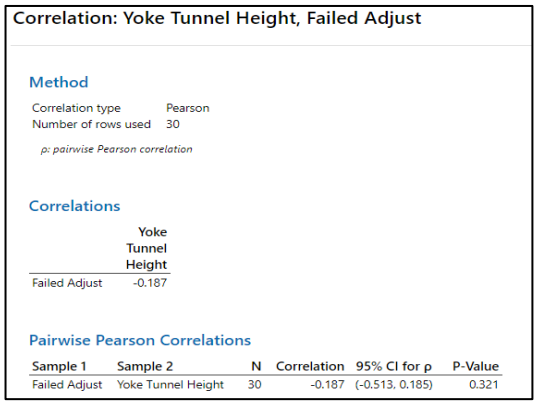

Fig 37: Pairwise Pearson Correlation Method Result for Yoke Tunnel Height and Failed Adjust (FA) Rejection

10.2.2 Humidity Fluctuations: Control Chart Analysis

The X-bar R control chart analysis of humidity over the past 78 days indicated that there were no points outside the control limits. This suggests that both the process mean and variation are stable and in control throughout the period. Therefore, the humidity process can be considered consistent and well-maintained.

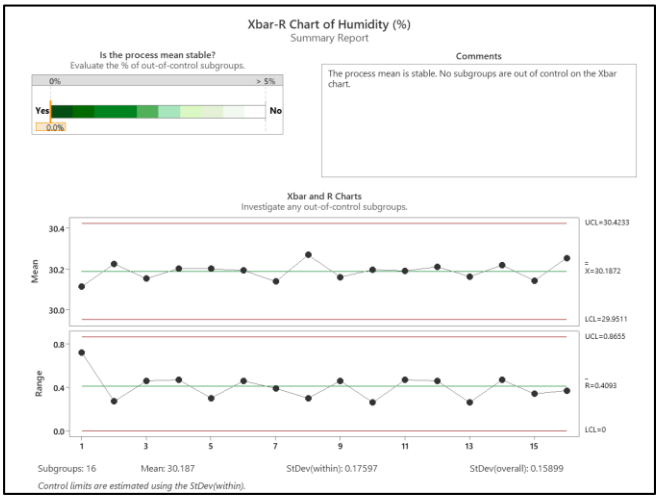

Fig 38: N=78 days Control Chart (X-bar R) Analysis: Humidity

10.2.3 Laser Welding Inconsistency: Weld Strength Control Chart Analysis

Laser welding consistency is directly correlated to pull strength (lb.f) based on statistical process control data. The X-bar and R control chart analysis for the pull test over the past two months showed no points outside the control limits. This indicates that both the process mean and variation are stable and in control throughout the period. Therefore, the laser welding process can be considered consistent and well-maintained.

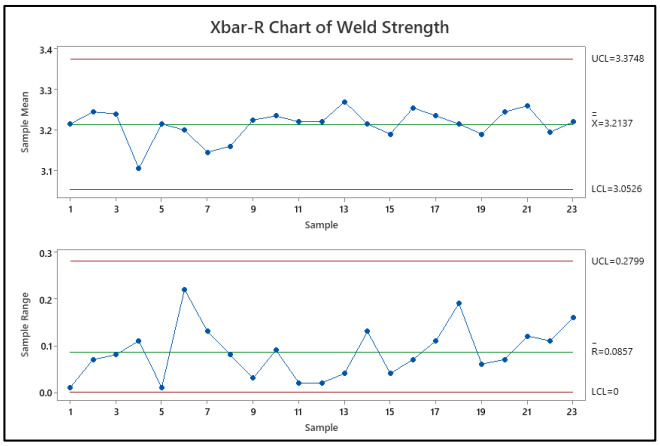

Fig 39: N=1 month Control Chart X-bar-R) Analysis: Weld Strength

10.2.4 Coupler Setup issues during adjustment and testing

The test configuration of Model X indicated on Knowles Test Specification Database System matches with the correct part number for Model X as shown in Figure 34.

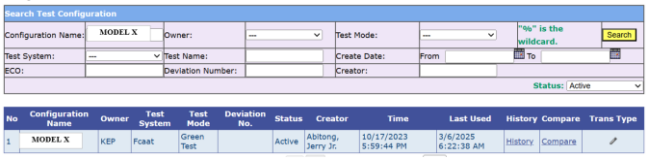

Fig 40: Test Specification Database System Result

10.2.5 MTC Machine Stability: Motor to Case Gap on Yoke Window

The motor-to-case gap on the yoke window is directly correlated to the stability of the motor-to-case welding machine. The X-bar and R control chart analysis for the motor-to-case gap on the yoke window over the past two months showed no points outside the control limits. This indicates that both the process mean and variation are stable and in control throughout the period. Therefore, the motor-to-case welding machine can be considered consistent and well-maintained.

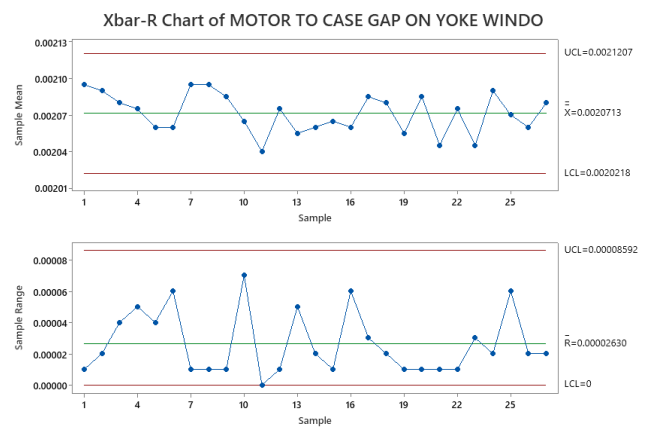

Fig 41: Control chart analysis of motor to case gap on yoke window

10.2. ESPC Measurement Error: Reed length Control Chart Analysis

Operator A's reed length measurements were analyzed using X-bar and R control charts, which showed no indications of process variation outside the control limits and no measurement errors, indicating a stable and in-control process.

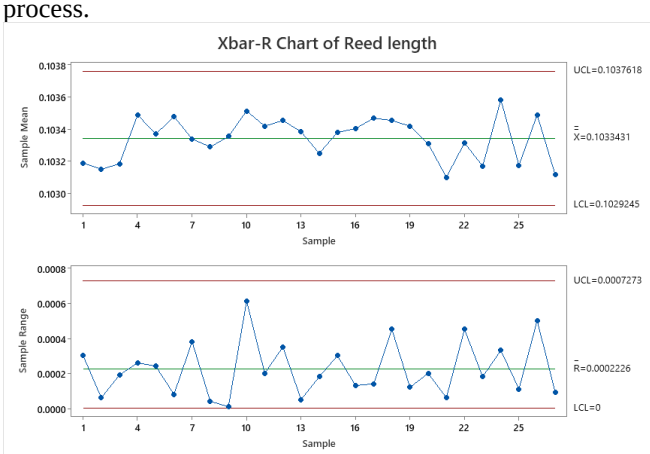

Fig 42: Control chart analysis of reed length to test measurement error (1 week data)